Island Arc (2007) **16,** 105–123

Research Article

Tectono-metamorphic history of the Tacagua ophiolitic unit (Cordillera de la Costa, northern Venezuela): Insights in the evolution of the southern margin of the Caribbean Plate

ALESSANDRO ELLERO,[1] ALESSANDRO MALASOMA,[2] MICHELE MARRONI,[1,2]* LUCA PANDOLFI[1,2] AND FRANCO URBANI[3]

[1]*Istituto di Geoscienze e Georisorse, CNR, Pisa,* [2]*Dipartimento di Scienze della Terra, Università di Pisa, Via S. Maria, 53, Pisa 56126, Italy (email: marroni@dst.unipi.it) and* [3]*Escuela de Geologia, Minas y Geofisica, Facultad de Ingeniería, Universidad Central de Venezuela, Caracas, Venezuela*

Abstract The southern margin of the Caribbean Plate is well exposed in the Cordillera de la Costa of northern Venezuela, where amalgamated terranes consisting of continental and oceanic units occur. In the Cordillera de la Costa, metamorphosed oceanic units crop out along the coast near Caracas. Among them, the Tacagua unit is characterized by metaserpentinites and metabasites showing mid-oceanic ridge basalt geochemical affinity. These lithologies, representative of a disrupted ophiolite sequence, are associated with metasediments consisting of calcschists alternating with pelitic and psammitic schists, whose protoliths were probably represented by deep-sea hemipelagic and turbiditic deposits. In the Tacagua unit, a polyphase deformation history has been reconstructed, consisting of four folding phases from *D1* to *D4*. Geological setting suggests an involvement of the Tacagua unit in the processes connected with a subduction zone. The following deformations (from *D2* to *D4*) observed in the field might be related to the exhumation history of the Tacagua unit. The late deformation history consists of an alternation of deformation phases characterized by displacement parallel (*D2* and *D4* phases) and normal (*D3* phase) to plate boundary between the Caribbean and South America Plates. All lines of geological evidence suggest that the whole evolution of the Tacagua unit was acquired in a setting dominated by oblique convergence, in which alternation of strike-slip and pure compressional or pure extensional tectonics occurred through time.

Key words: Caribbean Plate, oblique convergence, ophiolite, Tacagua unit, Venezuela.

INTRODUCTION

Ophiolites preserved as deformed and metamorphosed slices in collisional belts are regarded as fundamental markers for geodynamic reconstrunctions. The Caribbean area displays well-developed ophiolitic sequences, mainly at the southern and northern margins of the Caribbean Plate where collisional belts of Alpine age crop out. These ophiolite sequences are interpreted as remnants of the proto-Caribbean oceanic basin developed after the breakup of the Pangea in the Jurassic-Early Cretaceous timespan and subsequently involved in the Eo-Caribbean tectonic events of 'mid' Cretaceous-Early Tertiary age (e.g. Talukdar & Loureiro 1982; Dengo 1985; Burke 1988; Pindell *et al.* 1988; Pindell & Barrett 1990; Meschede & Frisch 1998; Giunta *et al.* 2002, 2003). Both these margins have been characterized by a long-lived tectonic history achieved in an oblique setting, in which events of subduction, accretion and exhumation were developed. Recently, different models for the subduction and exhumation processes in oblique convergent setting have been proposed by many authors (e.g. Avé Lallemant & Guth 1990; Giunta *et al.* 2002 and references therein).

*Correspondence.

Received 22 March 2004; accepted for publication 15 June 2006.

doi:10.1111/j.1440-1738.2007.00561.x

In this framework, the structural and metamorphic features of the ophiolitic sequence from the southern margin of the Caribbean Plate are able to provide valuable constraints for the geodynamic reconstructions of oblique convergent margins, which can be used to test the proposed models for the subduction and exhumation processes in this type of geodynamic setting.

In the current study, we present the reconstruction of the tectono-metamorphic history of the Tacagua unit from the southern margin of the Caribbean Plate (Cordillera de la Costa, northern Venezuela), mainly by structural and microstructural analyses and metamorphic petrologic investigations. The implications of the present study for the tectonic history of subduction and exhumation processes in an oblique convergent margin are also discussed.

GEOLOGICAL SETTING

The Caribbean Plate is a small microplate located between the South and North America Plates (Fig. 1). The northern and southern margins are both represented by wide, up to 300 km strike-slip shear zones that divide the Caribbean Plate from the North and South American Plates. The eastern and western margins consists in turn of active subduction systems where the oceanic lithosphere, belonging to the Atlantic Ocean in the east and to the Pacific Ocean in the west, subduct under the Caribbean Plate. In the inner zones, the Caribbean Plate is mainly represented by undeformed and very thick oceanic and/or transitional lithosphere of probably Cretaceous age, which were formed during the spreading between North and South America (Mauffrét & Leroy 1997; Sinton *et al.* 1998; Révillon *et al.* 2000). However, fragments of thinned continental crust derived from the North and South American Plates are also included in its borders (e.g. Meschede & Frisch 1998; Kerr *et al.* 1999; Giunta *et al.* 2003).

The southern and the northern margins of the Caribbean Plate consist of an Alpine Orogenic Belt represented by an assemblage of terranes separated from each other by dextral and sinistral strike-slip faults. These terranes preserve records of a complex geodynamic history (e.g. Talukdar & Loureiro 1982; Dengo 1985; Dengo & Case 1990; Stephan *et al.* 1990; Frisch *et al.* 1992; Giunta 1993; Iturralde 1994; Meschede & Frisch 1998; Giunta *et al.* 2002; Ostos *et al.* 2005), starting with the breakup of Pangea and followed by the development of a wide oceanic basin of Jurassic age, i.e. the proto-Caribbean Basin, probably connected with the western Tethys (Auboin *et al.* 1977). In the Cretaceous period, this basin was affected by an intraoceanic subduction leading to development of wide fore- and back-arc oceanic basins as well as island arcs. Since 'Mid' Cretaceous, the evolution of the Caribbean area has been dominated by eastward motion of the Caribbean plateau. In this setting, the pre-existing oceanic and back/fore-arc

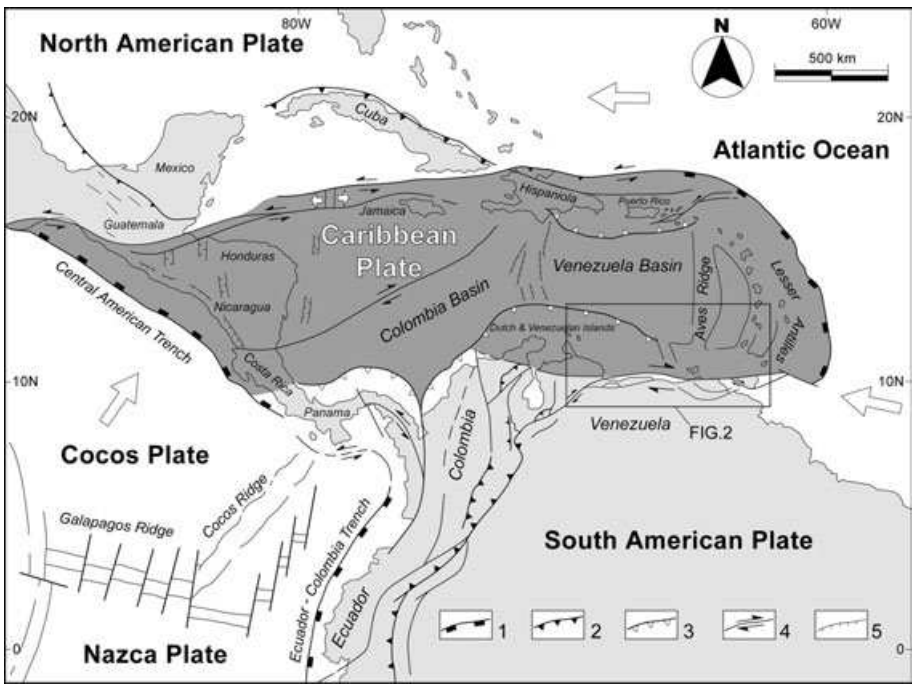

Fig. 1 Tectonic sketch of the Caribbean Plate. Arrows indicate the prevalent directions of the plate movements. The main active tectonic features are also shown: (1) trenches and subduction zones; (2) frontal thrusts; (3) Tertiary accretionary wedge; (4) strike-slip faults; (5) extensional faults (modified after Giunta *et al.* 2003).

basins were deformed during the 'Mid' Cretaceous and the Early Tertiary orogenic events ('EoCaribbean phase'). In this picture, both the northern and southern boundaries of the Caribbean Plates became characterized by lateral displacement leading to large-scale oblique convergence. Their history was largely controlled by strike-slip faults connected with a progressive eastward shifting of the Caribbean Plate. This tectonic evolution led to the development of multiple terranes, mainly located in the southern margin of the Caribbean Plate and consisting of amalgamated oceanic and continental units (e.g. Audemard & Audemard 2002).

The southern margin of the Caribbean Plate is today well exposed on land in the Northern Cordillera of Venezuela, where several terranes characterized by deformed and metamorphosed oceanic- and continental-derived units crop out (Fig. 2). According to Ellero *et al.* (2001), Giunta *et al.* (2002), Urbani and Rodríguez (2003) and Ostos *et al.* (2005), the identified terranes in the

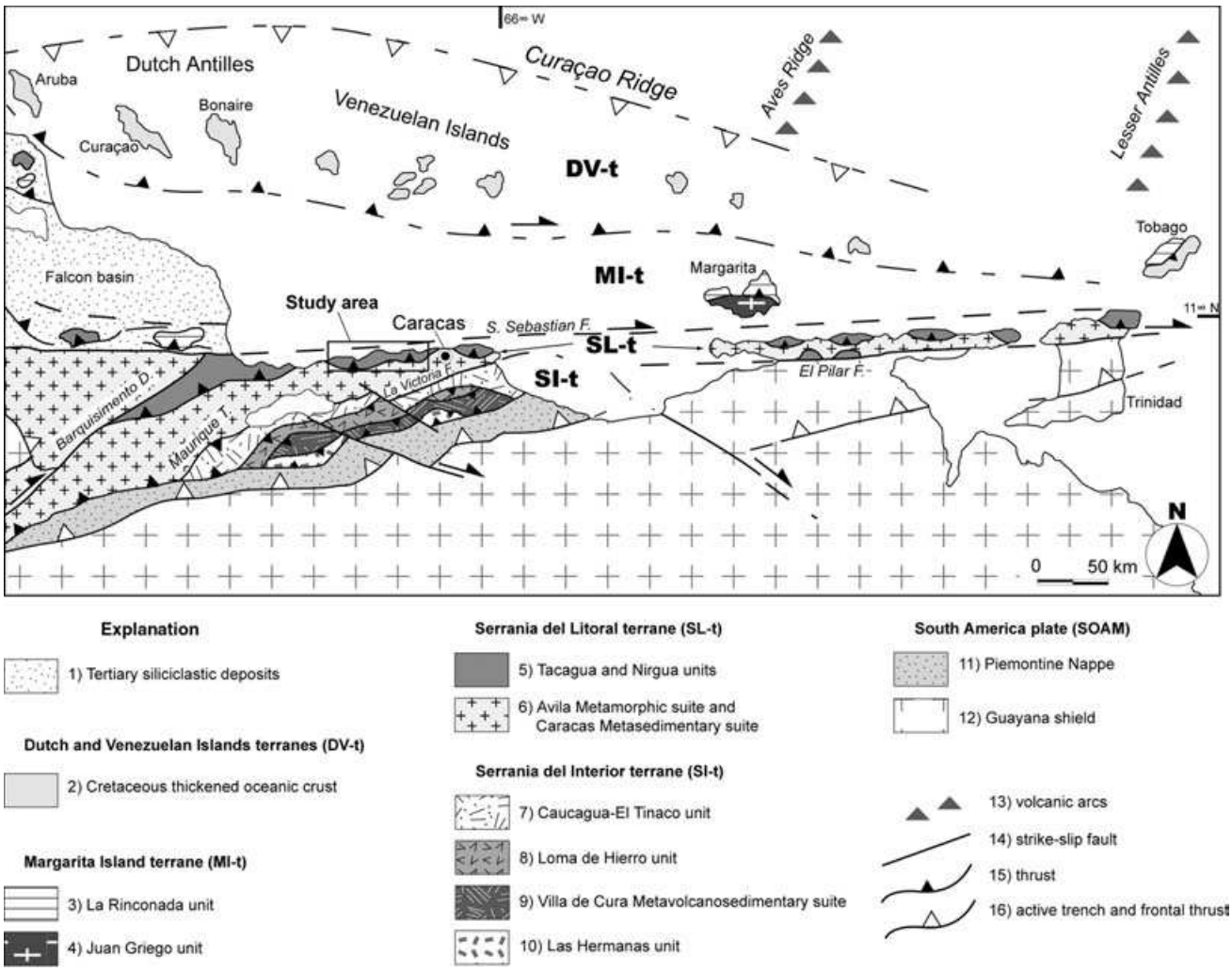

Fig. 2 Geological sketch map of the southern margin of the Caribbean Plate (modified after Giunta *et al.* 2003). (1) Tertiary siliciclastic deposits. Dutch and Venezuelan Islands terranes (DV-t). (2) Cretaceous thickened oceanic crust, and scattered sedimentary covers, intruded by Late Cretaceous calc-alkaline magmatism. Margarita Island terrane (MI-t). (3) Subcontinental mantle peridotites, layered gabbros, and doleritic dykes with Within Plate Tholeiitic (WPT) affinity (La Rinconada unit). (4) Paleozoic orthogneiss, paragneiss and schists (Juan Griego unit). Serrania del Litoral terrane (SL-t). (5) Late Jurassic-Early Cretaceous high pressure-low temperature mid-oceanic ridge basalt ophiolitic (MORB) units (Tacagua and Nirgua units). (6) Precambrian-Paleozoic orthogneiss, Late Jurassic-Cretaceous paragneiss, marbles, and schists (Cordillera de la Costa group). Serranía del Interior terrane (SI-t). (7) Subcontinental mantle peridotites, layered gabbros, pre-Mesozoic high-grade gneiss, Cretaceous volcano-sedimentary meta-sequence with WPT affinity (Caucagua- El Tinaco unit). (8) Late Jurassic-Early Cretaceous MORB ophiolites and related sedimentary covers (Loma de Hierro unit). (9) 'mid' Cretaceous HP/LT island arc sequences with Island Arc Tholeiitic (IAT) affinity (Villa de Cura unit). (10) 'Mid' Cretaceous island arc volcanics with IAT affinity (Dos Hermanas unit). South America Plate (SOAM). (11) Late Cretaceous-Paleocene terrigenous flysch sequences (Piemontine nappe). (12) Pre-Mesozoic continental crystalline basement and Mesozoic sedimentary covers (Guayana shield). Symbols. (13) Volcanic arcs of the Aves-Lesser Antilles system. (14) Strike-slip fault. (15) Thrust. (16) Active trench and frontal thrust.

Northern Cordillera of Venezuela are, from north to south, respectively: Dutch and Venezuelan Islands terrane, Margarita Island terrane, Serranía del Litoral terrane and Serranía del Interior terrane.

Sandwiched between the Margarita Island and Serranía del Interior terranes, the Serranía del Litoral terrane, bounded by two main dextral strike-slip faults, the San Sebastian fault to the north and La Victoria fault to the south (Fig. 2), is characterized by three east–west-trending belts (Urbani 1999; Urbani & Rodríguez 2003): (i) a coastal fringe of dismembered metamorphosed and deformed ophiolite sequences with mid-oceanic ridge basalt (MORB) affinity belonging to the Cretaceous rocks of the La Costa Metamorphic Suite, with mafic rocks showing high pressure (HP) mineral assemblages; (ii) a central belt showing a structure consisting of an map-scale antiform showing at the core Paleozoic and Precambrian rocks of the Ávila Metamorphic Suite, represented mainly by metasediments and metagranitic rocks deformed under epidote-amphibolite and amphibolite facies metamorphism; and (iii) a southern belt formed by the Late Jurassic-Early Cretaceous of the Caracas Metasedimentary Suite (formerly Caracas Group) unconformably covering the Silurian Sebastopol Gneiss. On the whole, the Ávila and Caracas suites are interpreted as representative of a continental margin and related sedimentary cover.

During the Cretaceous period, these sequences underwent deformation associated with greenschist facies metamorphism (Ostos 1990). Available K–Ar radiometric dating (Ostos 1990) yields ages from 79 to 30 Ma, and fission track apatite ages indicate ages range from 24 to 16 Ma.

According to Urbani and Rodríguez (2003), the La Costa Metamorphic Suite consists mainly of Tacagua Schist, Nirgua complex and unnamed serpentinite bodies. In the present study, a subdivision of The La Costa Metamorphic Suite in two tectonic units, named the Tacagua and Nirgua units, is proposed. Each unit is characterized by its own lithostratigraphic succession and different tectono-metamorphic history. The lithostratigraphic successions are represented by strongly deformed and metamorphosed rocks with mafic and ultramafic protoliths associated with pelitic and carbonaceous sedimentary deposits. The mafic and ultramafic rocks belong to an ophiolite sequence with MORB magmatic affinity interpreted as an ophiolitic fragment of the Proto-Caribbean Jurassic oceanic lithosphere successively involved in a subduction zone during the Late Cretaceous period (Beccaluva *et al.* 1996; quoted references).

The geological data available for the Tacagua unit are mainly provided by Talukdar and Loureiro (1982). In the Serranía del Litoral terrane, these authors have described a metamorphic sequence (referred to as Tacagua nappe) characterized by metasedimentary rocks affected by greenschists facies metamorphism and devoid of minerals indicative of HP conditions. The Tacagua nappe of Talukdar and Loureiro (1982) includes the Tacagua unit described in the current study, distinguished from the surrounding metamorphic sequences belonging to the Nirgua unit by a different metamorphic grade. Whereas the information about the tectono-metamorphic history of the Tacagua unit is very poor, more data are available for the Nirgua unit. This unit displays a more strongly deformed and metamorphosed ophiolite sequence, mainly represented by eclogite facies ultrabasic and basic rocks, associated with marbles, which in turn interfinger with gneisses and calcschists (Talukdar & Loureiro 1982; Beccaluva *et al.* 1996; Sisson *et al.* 1997). The eclogites of the Nirgua unit in Puerto Cabello, located 100 km west of the study area, consist mainly of relics of eclogites (*D1*a phase of Sisson *et al.* 1997) indicating approximately 1.8–2.2 GPa and 500°–700°C conditions (Sisson *et al.* 1997). These rocks occurs as boudins in a matrix characterized by a main foliation developed under epidote-amphibolite facies metamorphic conditions (*D1*c phase of Sisson *et al.* 1997). East–west-trending mineral and stretching lineations, as well as rootless, isoclinal folds are associated with the main foliation. The main foliation is, in turn, deformed to form close to isoclinal, overturned folds characterized by a well-developed crenulation cleavage (*D1*d and *D1*e phases of Sisson *et al.* 1997). This cleavage, recognized everywhere as a subhorizontal foliation, developed under greenschist facies metamorphic conditions. A subsequent phase, mainly distinguished by brittle structures, affects all the preexisting structures (*D2*a and *D2*b phases of Sisson *et al.* 1997). On the whole, the Nirgua unit is characterized by a metamorphic peak under eclogite-facies conditions followed by a retrograde evolution. These data are coherent with an interpretation of the Nirgua unit as oceanic fragments involved in an intraoceanic subduction zone and subsequently exhumed (Sisson *et al.* 1997). As a result of the presence of suitable lithologies, the radiometric ages are available only for the Nirgua unit. An $^{40}Ar/^{39}Ar$ age on white micas of *ca* 85 Ma

(Santonian) for the epidote-amphibolite metamorphism (*D1*c phase) has been provided by Avé Lallemant (1997). In addition, $^{40}Ar/^{39}Ar$ ages on white micas suggest 35–37 Ma (Middle to Late Eocene) for the greenschist facies metamorphism (*D1*d and *D1*e phases) (Smith *et al.* 1999). Fission-track zircon and apatite dating yields ages of *ca* 20 and *ca* 15 Ma (Burdigalian to Langhian), respectively (Sisson *et al.* 1997). These data suggest that the Nirgua unit experienced high pressure-low temperature metamorphism before the Santonian, followed by a long-lived history of exhumation from Santonian up to Langhian.

THE TACAGUA UNIT

STRATIGRAPHY

Despite the pervasive deformation and the associated metamorphism, a stratigraphic log of the Tacagua unit can be tentatively reconstructed from field evidence. In the core of the map-scale antiformal structures, large bodies of metaserpentinites, representing the base of the ophiolitic sequence, are still preserved, as recognized between Puerto Caracaya and Pta Diarima. In addition, rare outcrops of coarse-grained metabasites have been recognized close to the metaserpentinites. The largest outcrops of these rocks have been identified near Taguao. The most widespread metabasic rocks are represented by fine-grained metabasites. In some outcrops ellipsoidal bodies surrounded by epidote-rich layers probably represent former pillow lavas flattened parallel to the main foliation. On the whole, the collected data suggest that the Tacagua unit was characterized by a complete oceanic sequence ranging from serpentinites to gabbros and basalts (Méndez & Navarro 1987; Beccaluva *et al.* 1996; Giunta *et al.* 2002) topped by a monotonous succession made up of calcschists alternating with pelitic and psammitic schists, whose protoliths, probably represent deep-sea hemipelagic and turbiditic deposits (Urbani 1999). According to Beccaluva *et al.* (1996), the sequence of the Tacagua unit is generally regarded as consisting of a Jurassic ophiolite sequence topped by an Early Cretaceous sedimentary cover.

STRUCTURAL ANALYSES

The proposed deformation history of the Tacagua unit is based on detailed geological mapping associated with structural analyses carried out along the coast near Caracas, from Arrecife to Chichiriviche (Fig. 3). Along the cliffs, good exposures allow detailed observations on the structural setting of the Tacagua unit. Within the Tacagua unit a complex deformation history consisting of four distinct folding phases (hereafter referred to as *D1*, *D2*, *D3* and *D4* in chronologic order) has been recognized.

In the field, very few relics of the *D1* phase can be identified. These relics are mainly represented by quartz veins and very rare isoclinal, intrafolial and rootless folds with similar geometry and angular hinges. Both quartz veins and isoclinal F1 folds are deformed by F2 folds. By contrast, the structures of the *D2* phase are widespread at the mesoscale. This phase is characterized by similar, isoclinal folds, belonging to the classes 2 and 3 of the Ramsay (1967) classification, with thickened hinges and thinned limbs. The limbs are generally affected by boudinage, necking and pinch-and-swell structures. The F2 folds, rarely rootless, are characterized by hinges ranging from acute to subacute. Interbedded quartz- or calcite-rich layers display a more rounded hinge profile. The A2 fold axes are scattered, with azimuths ranging from N60E to N120E (Fig. 4a). This distribution can be related to the non-cylindrical nature of F2 folds and/or to the reorientation by later folding stage.

The F2 folds are characterized by a well-developed axial-planer continuous foliation, generally parallel to the lithological layers. In all the lithologies the S2 foliation represents the most pervasive and penetrative tectonic surface observed in the field (Fig. 5a). Shear sense indicators such as σ-type tails around boudinaged quartz veins are common in the field (Fig. 5b). After removing the effect of subsequent deformations, the sense of asymmetry indicates a top-to-the-northeast sense of shear. In the whole mapped area, the east–west-trending S2 foliation is generally subvertical or steeply inclined toward the north (Fig. 4c).

On the S2 foliation, the mineral lineation L2 is represented by elongate chlorite, white mica and amphibole grains and stretching lineations (mainly observed in the calcschists) and are represented by boudinaged millimetric pyrite and quartz grains with oriented growth of quartz fibers. Both mineral and stretching lineations display a preferred orientation showing a dominant N60E trend (Fig. 4b). The stretching-mineral lineations formed during the *D2* phase are considered to be parallel to the shearing direction.

The structures related to *D2* phase are everywhere deformed by the *D3* phase structures. This

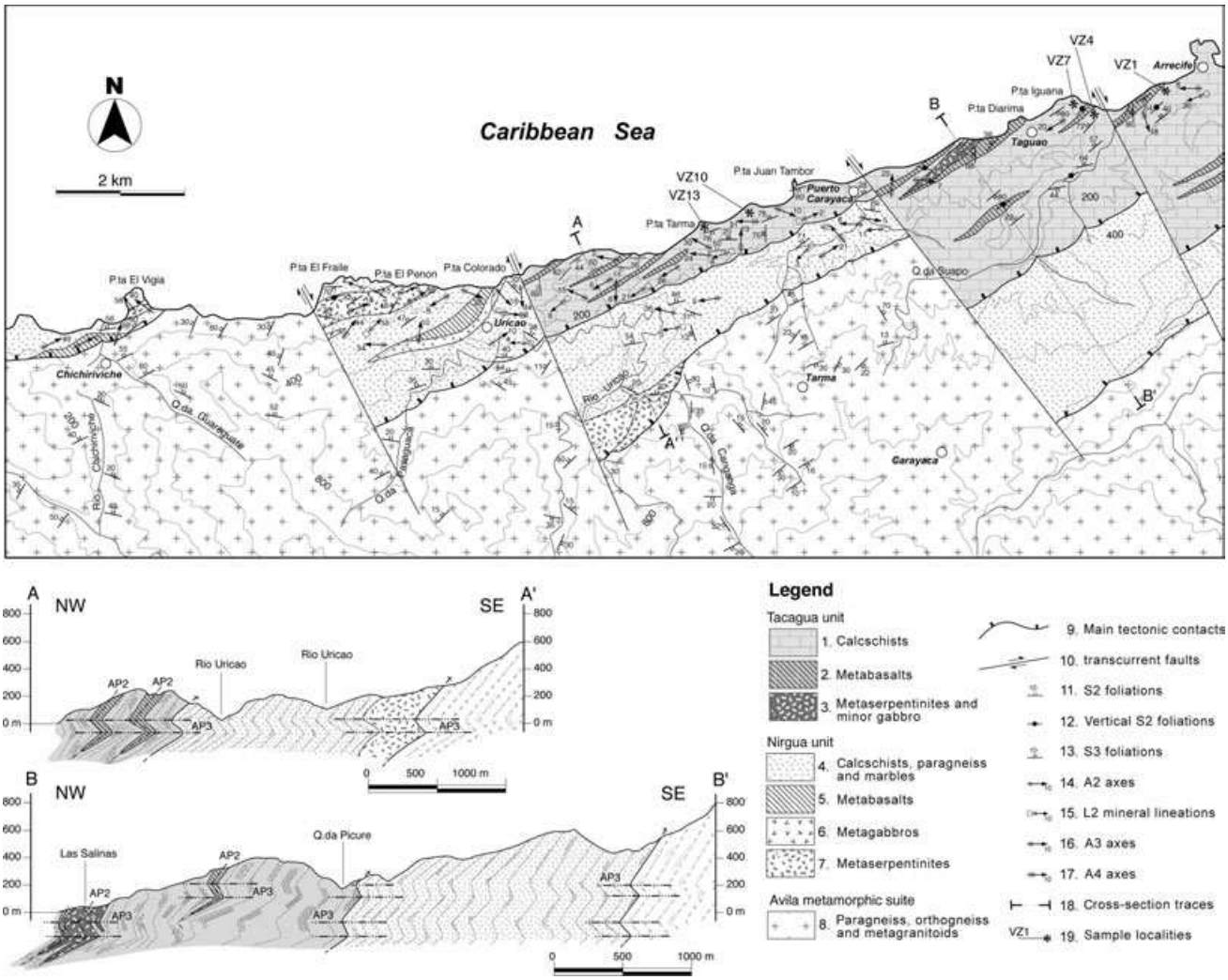

Fig. 3 Geological map of the Tacagua unit between Arrecife and Chichiriviche (Cordillera de la Costa, Venezuela) and geological cross-sections. The axial plane surfaces of *D2* (AP2) and *D3* (AP3) phases are indicated in the geological cross sections.

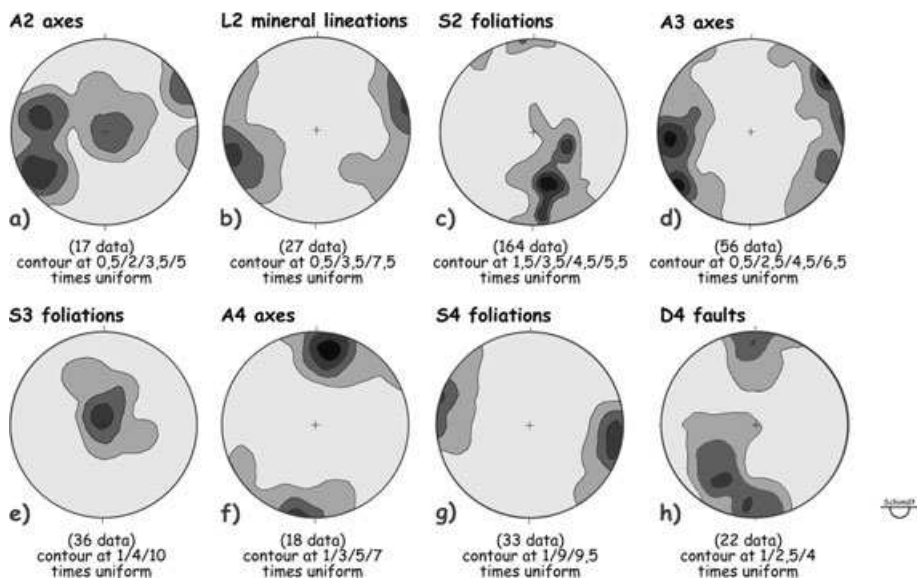

Fig. 4 Contour diagram of equal-area, lower hemisphere stereographic representation of structural data from Tacagua unit. In the diagrams c, e, g and h the pole of the planes are reported. For each diagram, the values of contour lines are reported as percentage of the total data per 1% area. Contour method after Rowland and Duebendorfer (1994).

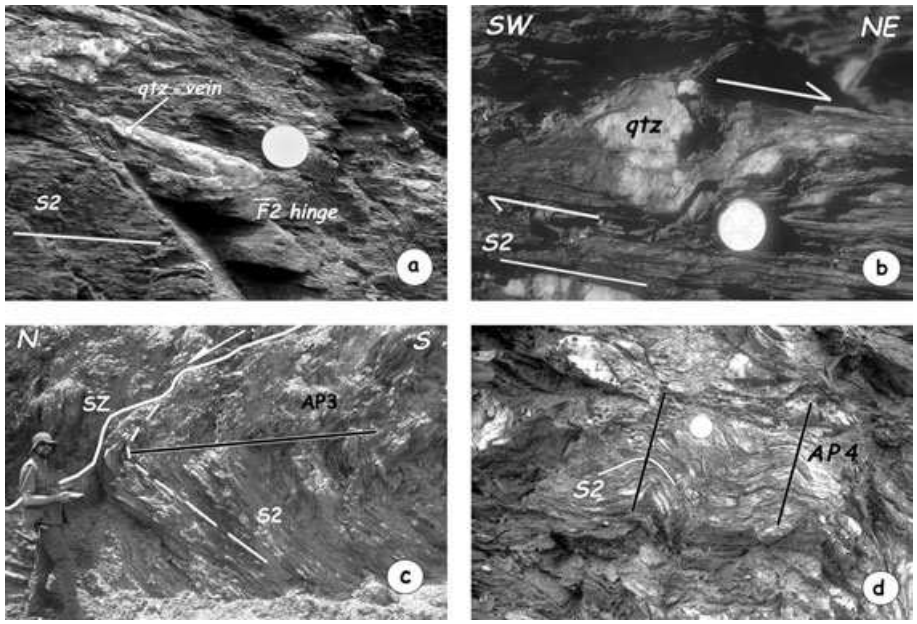

Fig. 5 Deformation features of the metasedimentary rocks of Tacagua unit: (a) quartz vein deformed by the *D2* phase into rootless, isoclinal folds with thickened hinge zone; (b) shear sense indicator represented by σ-type tails around boudinaged quartz veins along the S2 foliation; (c) F3 fold with subhorizontal AP3 axial plane and associated shear zone (SZ). The S2 foliation is also indicated; (d) F4 folds with steep AP4 axial planes.

phase is characterized by subisoclinal to open F3 folds with parallel geometry (Fig. 5c). The hinges range from rounded to subrounded, whereas the limbs are rarely boudinaged. Hinge collapse of the F3 folds have been also detected. The A3 axes are characterized by a N90E to N60E trend, roughly parallel to A2 axes (Fig. 4d). The F3 folds are asymmetric with a northward vergence, whereas their axial planes are everywhere subhorizontal (Fig. 4e). The axial plane S3 foliation ranges from crenulation to fracture cleavage, mainly depending to the lithology where this foliation is developed. On the fold limbs north to northwest-striking quartz or calcite fibers and slickensides are quite common, according to a flexural slip folding mechanism. Associated with F3 folds, low-angle shear zones characterized by schistosité-cisaillement (S-C) structures are widespread. After removing the effect of the subsequent deformation phases, these shear zones show normal fault motion with a top-to-the- north/northwest sense of shear.

In the field, the distinction between *D2* and *D3* phase structures is made possible by their different relationships with the S2 main, continuous foliation, everywhere showing different morphology from the younger S3 one. In addition, the F2 and F3 folds can be easily distinguish by the different attitude of their axial plane, generally at high-angle for the F2 folds and subhorizontal for the F3 ones.

The *D2* and *D3* structures are deformed by the *D4* phase, mainly represented by open F4 folds with rounded hinges and subvertical axial planes (Fig. 5d). The interlimb angle range from 90° to 140°. The A4 axes show a N10E strike and subhorizontal plunge (Fig. 4f). The axial plane foliation occurs only as a subvertical fracture cleavage (Fig. 4g). The F4 folds probably developed in association with east–west dextral strike-slip faults (Fig. 4h).

The map scale structures identified in the field are represented by kilometric isoclinal folds with metaserpentinites or metabasalts at the core. These structures can be related to the *D2* phase, because the folds are deformed by the F3 folds. The F3 folds are characterized by axes with the same orientation as the F2 folds, but showing low-angle axial planes, with type 3 interference patterns (Ramsay 1967) (cross-sections in Fig. 3). The tectonic boundary between the Tacagua and Nirgua units is deformed by the *D3* phase.

PETROGRAPHY AND MICROSTRUCTURAL ANALYSES

During the field mapping, oriented samples have been collected for microstructural analyses by optical microscope. The samples are representative of the deformation structures of all the phases identified in the field and they have been collected in all the lithological types from the Tacagua unit. Investigated samples consist mainly of calcschists, micaschists and psammitic schists, derived from the ophiolitic sedimentary cover. The calcschists are characterized by granoblastic layers consisting of calcite + quartz alternanting with lepidoblastic layers mainly composed by phyllosilicates (white mica + chlorite) + amphibole + quartz. The micaschists are very rich in phyllosilicates (white

mica + chlorite), arranged in thin lepidoblastic layers, in which two different foliations are recognizable. In the micaschists, granoblastic layers of quartz parallel to main foliation are also present. The psammitic schists are characterized by the presence of coarse-grained quartz, amphiboles and K-feldspar porphyroclasts wrapped by the main S2 foliation. Fine-grained porphyroclasts also occur in the micaschists and calcschists. In all the lithologies, the quartz-rich layers are characterized by strong dynamic recrystallization with a grain shape preferred orientation. Relict large quartz grains with a ductile intracrystalline deformation are also present.

Different mineral assemblages are linked to the deformation microstructures of the different phases. In thin sections, the most pervasive anisotropy is represented by the S2 foliation, generally crenulated by the following S3 foliation. However, relics of the S1 foliation can be also observed, more easily in the thin sections from the hinge zone of the F2 folds in the calcschists, the micaschists and in the psammitic schists (Fig. 6a). In these zones, the S1 foliation occurs everywhere as a relic and transposed foliation, only observed in the microlithons. The S1 foliation occurs as a well-developed and continuous anisotropy, that can be defined as a schistosity. Locally, the S1 foliation wraps the fine-grained quartz and K-feldspar porphyroclasts. In these lithologies, relics of the minerals developed during the *D1* phase are white mica, quartz, chlorite and clinozoisite. In thin sections, the quartz veins show antitaxial structures characterized by well-developed fibers and median lines. These structures, well-developed in the calcschists, are referred to the *D1* phase. The metabasalts as well as the metaserpentinites are devoid of mineralogic relics of the *D1* phase.

The S2 foliation is the most continuous and pervasive anisotropy in all the studied rocks. In thin sections, the psammitic schists, the micaschists and the calcschists are characterized by a S2 foliation classified as continuous penetrative schistosity (Fig. 6b) characterized by parallel, synkinematic grains of white mica, quartz, calcite, chlorite, albite, hematite, epidote, amphibole and titanite. The kinematic indicators, mainly σ-type porphyroclasts of quartz and amphibole, suggest a top-to-northeast sense of shear. The same sense of shear is provided by synthetic and antithetic microfaults in large porphyroclasts. Recrystallized tails of quartz, amphibole and albite have been also observed, mainly around large porphyroclasts of quartz and feldspar (Fig. 6c). In the metabasalts the S2 foliation consists of a continuous schistosity defined by oriented minerals of albite, amphibole, chlorite and epidote.

In the psammitic schists and calcschists, the S2 foliation is generally deformed by the *D3* phase. The S3 foliation is represented by a pervasive anisotropy that is found in the schists and calcschists as parallel and zonal crenulation cleavage with discrete transition between cleavage domains and microlithons (Fig. 6d). In the metabasalts the S3 foliation is recognized as poorly developed and spaced crenulation cleavage characterized by a discrete transition between cleavage

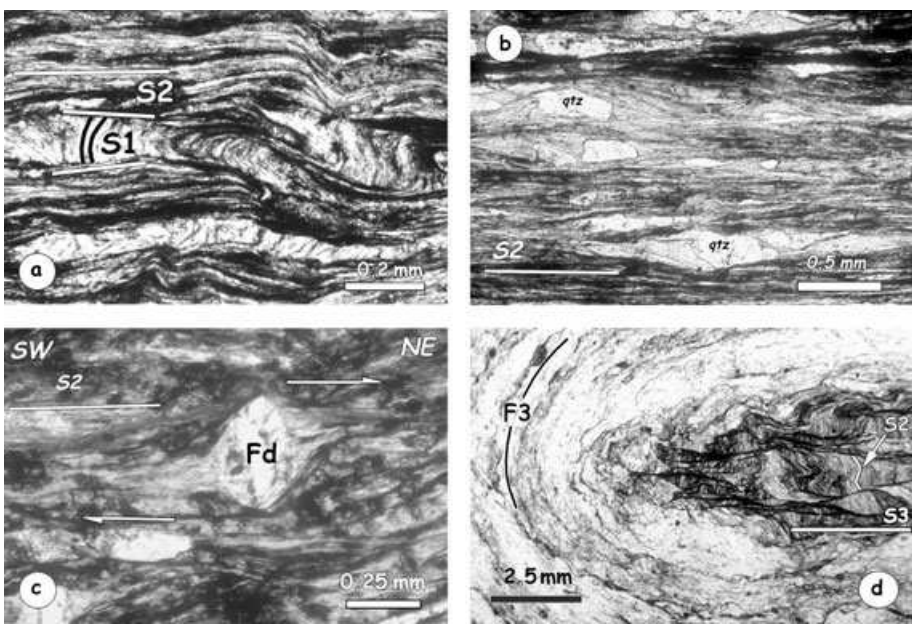

Fig. 6 Microphotographs of metasedimentary rocks from Tacagua unit: (a) relationships between the S1 and S2 foliations in the calcschists. The minerals identified in the relic S1 foliation inside the microlithons are represented by phengites with high celadonitic content and quartz, whereas the S2 foliation is characterized by chlorite, phengite with low celadonitic content, quartz and Fe-oxides; (b) S2 foliation in fine-grained calcschists (see text for explanation); (c) σ-type porphyroclast of K-feldspar, with recrystallized tails of albite, amphibole and albite; (d) Hinge zone of F3 fold characterized in the fine grained layer by a S3 anastamozing crenulation cleavage, that does not affect the quartz-rich layer.

domains and microlithons. During the *D3* phase the main deformation mechanism is represented by pressure solution and reorientation of pre-existing tabular grains. However, minor recrystallization of quartz, calcite and Fe-oxides also occurs. Recrystallized crystals of calcite show twins belonging to Type 1 and 2 of Burkhard (1993) classification.

In all the sampled lithologies, no pervasive syn-kinematic recrystallization is associated with the *D4* phase, whose structural features are coherent with deformation at very high structural level.

MINERAL CHEMISTRY

On the selected thin sections (Table 1), the chemistry of the minerals associated with the main foliations have been analyzed. The location of the samples are shown in Figure 3. Microanalytical studies on metamorphic assemblages were carried out using a JEOL JXA-8600 electron microprobe analyzer equipped with 4WD-spectrometers (C.N.R.-Istituto di Geoscienze e Georisorse, Firenze, Italy). Operating conditions were 15 kV accelerating voltage, 10 nA beam current, beam spots between 1 and 10 μm in diameter. The largest spots were used on alkali-rich minerals to avoid Na-K volatilization.

The *D1* metamorphic mineral assemblage includes white mica + chlorite ± quartz ± clinozoisite. From the *D1* mineral assemblage white mica, chlorite and clinozoisite have been analyzed by electron microprobe. White micas formulae were calculated assuming 11 oxygen and all Fe as Fe^{2+}. The presence of minor Fe^{3+} amounts results in a slight decrease of the Si cations in the formula unit, typically to <0.1 pfu. White micas from calcschists and micaschists have high amounts of Si and Mg (0.33–0.44 pfu) and can be classified as phengites. These phengites have Si contents between 3.42 and 3.49 pfu (Table 2). Chlorite formulae were calculated assuming 14 oxygen and all Fe as Fe^{2+}. For clinozoisite the formulae were calculated on the basis of 12.5 oxygen and assuming all Fe as Fe^{3+}. Clinozoisite from calcschists contains low amounts of Fe^{3+} and Ca contents between 2.02 and 2.09 pfu (Table 2). The pistacite component ($Fe^{3+}/(Fe^{3+} + Al^{3+})$) in *D1* clinozoisites ranges between 0.03 and 0.11.

The *D2* metamorphic mineral assemblage is: white mica + quartz ± calcite ± chlorite ± albite ± amphibole ± epidote ± hematite ± titanite. From the *D2* mineral assemblage white mica, amphibole and epidote have been analyzed by electron microprobe. The *D2* white micas (on the basis of 11 oxygen and all Fe as Fe^{2+}) have a lower celadonite content, with Si amounts between 3.06 and 3.27 pfu (Table 3). White micas have variable Mg content (0.09–0.33 pfu). For amphiboles the formulae were calculated assuming 23 oxygen and classification of Leake *et al.* (1997) was adopted (Fig. 7). Site assignment and ferric iron content in amphiboles was calculated using the estimation proposed by Schumacher in Leake *et al.* (1997). Amphiboles are calcic and characterized by an anhedral core of Mg-hornblende with an overgrowth of actinolite (Si: 7.55–7.97 pfu) (Table 4). The actinolitic rim has often an euhedral shape. Finally, epidotes formulae were calculated on the basis of 12.5 oxygen and assuming all Fe as Fe^{3+}. Each analyzed crystal does not show any compositional zoning. Despite this, the epidotes from the *D2* phase have a Fe^{3+} amount ranging from 0.42 to 0.53 pfu. The Fe^{3+} amounts are higher, if compared with clinozoisites from the *D1* metamorphic mineral assemblage (Table 3).

ESTIMATE OF METAMORPHIC CONDITIONS

The pressure–temperature condition of *D1* metamorphic assemblage are constrained by the association of phengite (Si: 3.42–3.43 pfu in the sample VZ10) + chlorite + quartz ± clinozoisite. The temperature range is constrained by the temperature of crystallization of chlorites from the *D1* phase. The temperature conditions can be estimated using the Chl + Qtz reaction curve (clinochlore + sudoite = Mg-amesite + quartz + H_2O). The used

Table 1 Selected samples for mineral chemistry analyses

Sample	Lithology	*D1* assemblage	*D2* assemblage
VZ1	Micaschist	Phe + Chl	Phe + Qtz + Am + Ep
VZ4	Micaschist		Phe + Chl + Qtz + Am + Ep + Ab + Cal + Ttn + Hem
VZ7	Calcschist	Phe + Chl	Phe + Chl + Qtz + Am + Ep + Hem
VZ10	Calcschist	Phe + Chl + Qtz + Czo	Phe + Chl + Qtz + Ab + Cal + Ttn
VZ13	Micaschist	Phe + Chl + Qtz	Phe + Chl + Qtz + Hem

The relevant lithology and the metamorphic mineral assemblages associated with *D1* and *D2* deformation phases are also given.

Table 2 Analyses of representative phengites (on the basis of 11 oxygen and all Fe as Fe^{2+}), chlorites (on the basis of 14 oxygen and all Fe as Fe^{2+}) and clinozoisites (on the basis of 12.5 oxygen and all Fe as Fe^{3+}) from *D1* mineral assemblages

Sample	VZ4 Phe2	VZ4 Phe3	VZ7 Phe1	VZ7 Phe2	VZ7 Phe3	VZ7 Phe4	VZ7 Phe6	VZ10 Phe3	VZ10 Phe5	VZ13 Phe3	VZ4 Chl1	VZ4 Chl2	VZ4 Chl3	VZ13 Chl1	VZ13 Chl2	VZ10 Chl1	VZ10 Czo1	VZ10 Czo2	VZ10 Czo3	VZ10 Czo4
Wt%																				
SiO_2	49.06	49.32	51.74	51.40	51.02	50.80	49.60	50.69	50.54	48.32	27.82	26.89	27.44	27.54	28.90	29.29	40.10	39.40	37.55	39.28
TiO_2	0.06	–	–	0.12	–	–	0.08	0.14	0.11	0.18	–	–	–	–	0.06	–	–	0.05	0.06	0.07
Al_2O_3	26.05	28.10	25.43	27.15	26.11	26.33	26.96	27.66	32.71	32.13	18.91	20.64	21.08	22.53	22.93	24.15	31.52	29.07	28.02	29.16
Cr_2O_3	0.12	0.07	–	–	–	–	–	0.10	–	–	0.20	–	–	0.09	–	0.08	–	–	–	–
FeO	3.39	2.44	3.32	3.14	2.91	3.23	2.93	1.37	0.86	2.66	20.97	21.00	20.42	25.09	25.49	11.48	1.49	4.83	3.88	4.10
MnO	–	–	–	–	–	–	0.08	–	–	0.05	0.35	0.30	0.34	0.29	0.30	0.09	–	0.10	–	–
MgO	3.97	3.34	4.38	3.75	3.68	3.95	3.49	3.32	2.21	1.52	18.79	18.09	18.12	11.29	10.49	21.77	–	0.06	0.08	–
CaO	0.12	0.09	0.04	–	–	–	0.04	–	–	–	0.11	0.07	0.17	0.22	0.25	–	24.68	24.31	22.59	24.33
Na_2O	0.12	–	0.09	–	–	–	0.09	0.25	0.35	0.51	–	–	–	0.24	0.29	–	–	–	–	–
K_2O	8.35	8.84	8.41	8.68	8.89	8.61	9.04	9.88	6.61	8.53	0.03	–	–	0.38	0.78	0.77	–	–	0.04	–
Total	91.24	92.20	93.41	94.24	92.61	92.92	92.31	93.41	93.39	93.90	87.18	86.99	87.57	87.67	89.49	87.63	97.79	97.82	92.22	96.94
Cations																				
Si	3.40	3.37	3.49	3.43	3.47	3.44	3.40	3.42	3.32	3.24	2.88	2.79	2.81	2.88	2.96	2.85	3.06	3.07	3.08	3.07
Al VI	0.60	0.63	0.51	0.57	0.53	0.56	0.60	0.58	0.68	0.76	1.12	1.21	1.19	1.12	1.04	1.15	0.00	0.00	0.00	0.00
Sum Z	4.00	4.00	4.00	4.00	4.00	4.00	4.00	4.00	4.00	4.00	4.00	4.00	4.00	4.00	4.00	4.00	3.06	3.07	3.08	3.07
Al IV	1.53	1.63	1.51	1.57	1.56	1.55	1.57	1.61	1.85	1.77	1.19	1.31	1.36	1.66	1.73	1.62	2.84	2.67	2.71	2.69
Ti	0.00	0.00	0.00	0.01	0.00	0.00	0.00	0.01	0.01	0.01	0.00	0.00	0.00	0.00	0.00	0.00	0.00	0.00	0.00	0.00
Cr	0.01	0.00	0.00	0.00	0.00	0.00	0.00	0.01	0.00	0.00	0.02	0.00	0.00	0.01	0.00	0.01	0.00	0.00	0.00	0.00
Fe^{3+}	0.00	0.00	0.00	0.00	0.00	0.00	0.00	0.00	0.00	0.00	0.00	0.00	0.00	0.00	0.00	0.00	0.10	0.31	0.27	0.27
Fe^{2+}	0.20	0.14	0.19	0.18	0.17	0.18	0.17	0.08	0.05	0.15	1.81	1.82	1.75	2.20	2.18	0.93	0.00	0.00	0.00	0.00
Mn	0.00	0.00	0.00	0.00	0.00	0.00	0.00	0.00	0.00	0.00	0.03	0.03	0.03	0.03	0.03	0.01	0.00	0.01	0.00	0.00
Mg	0.41	0.34	0.44	0.37	0.37	0.40	0.36	0.33	0.22	0.15	2.90	2.79	2.76	1.76	1.60	3.15	0.00	0.01	0.01	0.00
Sum Y	2.14	2.11	2.13	2.12	2.10	2.13	2.11	2.04	2.11	2.09	5.94	5.95	5.90	5.65	5.54	5.72	2.93	3.00	2.99	2.96
Ca	0.01	0.01	0.00	0.00	0.00	0.00	0.00	0.00	0.00	0.00	0.01	0.01	0.02	0.02	0.03	0.00	2.02	2.03	1.99	2.04
Na	0.02	0.00	0.01	0.00	0.00	0.00	0.01	0.03	0.04	0.07	0.00	0.00	0.00	0.05	0.06	0.00	0.00	0.00	0.00	0.00
K	0.74	0.77	0.72	0.74	0.77	0.74	0.79	0.85	0.55	0.73	0.00	0.00	0.00	0.05	0.10	0.10	0.00	0.00	0.00	0.00
Sum X	0.76	0.78	0.74	0.74	0.77	0.74	0.80	0.88	0.60	0.80	0.02	0.01	0.02	0.12	0.19	0.10	2.02	2.03	1.99	2.04
Total	6.91	6.89	6.87	6.86	6.87	6.88	6.91	6.92	6.71	6.88	9.96	9.95	9.92	9.77	9.73	9.81	8.02	8.09	8.06	8.08

–, below detection limit.

Table 3 Analyses of representative phengites (on the basis of 11 oxygen and all Fe as Fe^{2+}) and epidotes (on the basis of 12.5 oxygen and all Fe as Fe^{3+}) from *D2* mineral assemblages

Sample	VZ10 Phe1	VZ10 Phe4	VZ13 Phe4	VZ13 Phe5	VZ13 Phe6	VZ13 Phe8	VZ13 Phe10	VZ13 Phe11	VZ13 Phe12	VZ1 Ep1	VZ1 Ep2	VZ1 Ep3	VZ1 Ep4
Wt%													
SiO_2	48.88	48.20	47.78	47.36	45.96	47.00	48.75	45.50	43.63	39.69	38.57	39.42	38.66
TiO_2	0.10	–	0.17	0.22	0.20	0.14	0.18	0.09	0.23	0.09	0.07	0.05	0.08
Al_2O_3	32.51	31.94	33.48	34.77	36.39	35.04	30.98	31.02	32.74	26.03	27.56	28.37	28.31
Cr_2O_3	0.15	0.23	0.07	–	–	–	–	–	–	–	–	–	0.09
FeO	0.91	1.44	2.25	1.74	1.62	1.43	3.13	6.56	5.71	8.15	7.64	6.39	7.57
MnO	–	–	–	–	–	–	–	0.09	–	0.08	–	0.15	–
MgO	2.03	3.38	1.36	0.92	1.04	0.94	1.90	2.97	2.32	1.38	–	–	–
CaO	–	–	0.04	–	0.15	–	–	0.08	0.10	23.20	24.42	24.19	24.58
Na_2O	0.62	0.65	0.51	0.67	1.36	0.62	0.21	0.43	0.59	–	–	–	–
K_2O	9.27	8.64	8.76	8.75	7.10	8.62	8.91	7.32	6.92	–	–	–	–
TOT	94.47	94.48	94.42	94.43	93.82	93.79	94.06	94.06	92.24	98.62	98.26	98.57	99.29
Cations													
Si	3.24	3.20	3.18	3.15	3.06	3.14	3.27	3.11	3.02	3.11	3.04	3.07	3.02
Al VI	0.76	0.80	0.82	0.85	0.94	0.86	0.73	0.89	0.98	0.00	0.00	0.00	0.00
Sum Z	*4.00*	*4.00*	*4.00*	*4.00*	*4.00*	*4.00*	*4.00*	*4.00*	*4.00*	*3.11*	*3.04*	*3.07*	*3.02*
Al IV	1.78	1.70	1.81	1.87	1.91	1.89	1.72	1.60	1.69	2.41	2.56	2.60	2.60
Ti	0.00	0.00	0.01	0.01	0.01	0.01	0.01	0.00	0.01	0.01	0.00	0.00	0.00
Cr	0.01	0.01	0.00	0.00	0.00	0.00	0.00	0.00	0.00	0.00	0.00	0.00	0.01
Fe^{3+}	0.00	0.00	0.00	0.00	0.00	0.00	0.00	0.00	0.00	0.53	0.50	0.42	0.49
Fe^{2+}	0.05	0.08	0.13	0.10	0.09	0.08	0.18	0.37	0.33	0.00	0.00	0.00	0.00
Mn	0.00	0.00	0.00	0.00	0.00	0.00	0.00	0.01	0.00	0.01	0.00	0.01	0.00
Mg	0.20	0.33	0.13	0.09	0.10	0.09	0.19	0.30	0.24	0.16	0.00	0.00	0.00
Sum Y	*2.05*	*2.13*	*2.08*	*2.07*	*2.11*	*2.07*	*2.10*	*2.29*	*2.28*	*3.11*	*3.07*	*3.03*	*3.11*
Ca	0.00	0.00	0.00	0.00	0.01	0.00	0.00	0.01	0.01	1.95	2.06	2.02	2.05
Na	0.08	0.08	0.07	0.09	0.18	0.08	0.03	0.06	0.08	0.00	0.00	0.00	0.00
K	0.78	0.73	0.74	0.74	0.60	0.73	0.76	0.64	0.61	0.00	0.00	0.00	0.00
Sum X	*0.86*	*0.82*	*0.81*	*0.83*	*0.79*	*0.81*	*0.79*	*0.70*	*0.70*	*1.95*	*2.06*	*2.02*	*2.05*
TOT	*6.91*	*6.95*	*6.90*	*6.90*	*6.90*	*6.89*	*6.89*	*6.99*	*6.97*	*8.18*	*8.17*	*8.12*	*8.18*

–, below detection limit.

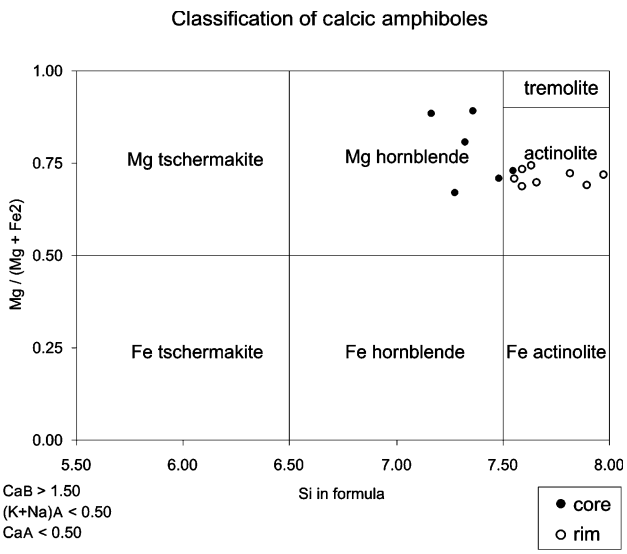

Fig. 7 Composition of calcic amphiboles. Classification after Leake *et al.* (1997) was adopted.

method is an exact calculation of the equilibrium temperature using chlorite composition and a fixed pressure (0.50 GPa in this case). The thermodynamic data and the chlorite solid solution model are from Vidal *et al.* (2001). The chlorite chemical analyses were selected using the criteria proposed by Vidal *et al.* (2001); these criteria were used to reject analyses that cannot be expressed as a linear combination of four end-member: (Fe-Mg)amesite (Fe-Mg)sudoite, clinochlore and daphnite. This thermometric method gives temperatures ranging between 339 and 406°C. The celadonite content (Si in formula) of phengite coexisting with quartz, K-feldspar and biotite is mainly dependent on pressure (Velde 1967; Massonne & Schreyer 1987; Massonne & Szpurska 1997). This geobarometric method can be applied to the studied rocks. However, the lack of biotite and K-feldspar in the assemblages means that the phengite compositions yield minimum pressure estimates. For the estimated temperatures range (339–406°C) the curves of phengitic substitution

Table 4 Analysis of representative calcic amphiboles from *D2* mineral assemblage. Structural formula is calculated assuming 23 oxygen. Site assignment and ferric iron content in amphiboles was calculated using the estimation proposed by Schumacher in Leake *et al.* (1997)

	Hbl2C	Hbl3C	Hbl4C	Hbl5C	Hbl7C	Act1C	Act1R	Act2R	Act3R	Act4R1	Act4R2	Act5R1	Act5R2	Act6R
Wt%														
SiO_2	49.58	52.45	51.33	51.40	50.95	52.57	52.60	54.50	55.62	52.81	54.91	51.60	52.58	52.37
TiO_2	0.77	0.54	0.63	0.37	0.71	0.47	0.24	–	–	0.80	–	0.24	0.23	0.35
Al_2O_3	5.34	4.20	6.20	4.19	5.10	3.21	2.86	1.65	0.67	2.49	0.80	2.61	2.81	2.78
Cr_2O_3	–	0.08	0.38	0.20	0.59	0.19	–	–	–	0.15	–	–	0.17	–
FeO	13.82	7.66	6.84	12.11	8.30	12.50	13.93	12.09	11.37	10.80	13.25	13.76	11.99	11.94
MnO	0.20	0.14	0.09	0.17	0.20	0.11	0.21	0.14	0.24	0.15	0.16	0.17	0.17	–
MgO	13.91	19.32	19.01	15.08	17.15	15.84	14.90	16.42	16.48	16.42	15.93	15.32	16.03	15.42
CaO	12.10	12.24	12.45	12.35	12.54	12.03	12.63	12.16	12.76	12.41	12.49	12.22	12.52	12.56
Na_2O	0.86	0.84	1.19	0.61	0.82	0.63	0.41	0.32	0.18	0.45	0.11	0.37	0.52	0.53
K_2O	0.15	–	0.06	–	0.05	–	–	–	–	0.07	–	–	–	0.11
Total	96.73	97.47	98.18	96.48	96.41	97.55	97.78	97.28	97.32	96.55	97.65	96.29	97.02	96.06
Cations														
Si	7.27	7.36	7.17	7.48	7.32	7.55	7.59	7.82	7.97	7.63	7.90	7.55	7.59	7.66
Al IV	0.73	0.64	0.83	0.52	0.68	0.45	0.41	0.18	0.03	0.37	0.10	0.45	0.41	0.34
Sum T	8.00	8.00	8.00	8.00	8.00	8.00	8.00	8.00	8.00	8.00	8.00	8.00	8.00	8.00
Al VI	0.20	0.05	0.19	0.20	0.19	0.09	0.08	0.10	0.08	0.06	0.03	0.00	0.07	0.14
Fe^{3+}	0.19	0.41	0.28	0.12	0.11	0.23	0.21	0.10	– 0.01	0.09	0.07	0.30	0.20	0.01
Ti	0.08	0.06	0.07	0.04	0.08	0.05	0.03	0.00	0.00	0.09	0.00	0.03	0.02	0.04
Cr	0.00	0.01	0.04	0.02	0.07	0.02	0.00	0.00	0.00	0.02	0.00	0.00	0.02	0.00
Mg	3.04	4.04	3.96	3.27	3.68	3.39	3.21	3.51	3.52	3.54	3.41	3.34	3.45	3.36
Fe^{2+}	1.49	0.43	0.46	1.34	0.89	1.22	1.48	1.29	1.38	1.21	1.48	1.33	1.24	1.45
Mn	0.00	0.00	0.00	0.00	0.00	0.00	0.00	0.00	0.03	0.00	0.00	0.00	0.00	0.00
Sum C	5.00	5.00	5.00	5.00	5.00	5.00	5.00	5.00	5.00	5.00	5.00	5.00	5.00	5.00
Mg	0.00	0.00	0.00	0.00	0.00	0.00	0.00	0.00	0.00	0.00	0.00	0.00	0.00	0.00
Fe^{2+}	0.02	0.06	0.05	0.01	0.01	0.05	0.00	0.06	0.00	0.01	0.04	0.06	0.01	0.00
Mn	0.02	0.02	0.01	0.02	0.02	0.01	0.02	0.02	0.00	0.02	0.02	0.02	0.02	0.00
Ca	1.90	1.84	1.86	1.93	1.93	1.85	1.95	1.87	1.96	1.92	1.92	1.92	1.94	1.97
Na	0.05	0.09	0.07	0.04	0.04	0.08	0.02	0.05	0.04	0.05	0.02	0.01	0.03	0.03
Sum B	2.00	2.00	2.00	2.00	2.00	2.00	2.00	2.00	2.00	2.00	2.00	2.00	2.00	2.00
Na	0.19	0.14	0.25	0.13	0.19	0.09	0.09	0.03	0.01	0.07	0.02	0.10	0.11	0.12
K	0.03	0.00	0.01	0.00	0.01	0.00	0.00	0.00	0.00	0.01	0.00	0.00	0.00	0.02
Sum A	0.22	0.14	0.26	0.13	0.20	0.09	0.09	0.03	0.01	0.09	0.02	0.10	0.11	0.14

–, below detection limit.

(Massonne & Szpurska 1997) provide a pressure higher than 0.45 GPa. Summing up the available geothermobarometric information, the *D1* metamorphic condition can be determined as 339°C < T < 406°C and P > 0.45 GPa.

The pressure-temperature condition of the *D2* metamorphic assemblage are constrained by the following association: phengite (Si: 3.06–3.27 pfu) + quartz ± calcite ± chlorite ± albite ± Fe-oxides (hematite) ± epidote ± Ca-amphibole (Mg-Hbl to Act) ± titanite. The Mg-hornblende stability field in hematite-bearing basic schists is indicative of a temperature higher than 400°C (Otsuki & Banno 1990). The pressure range provided by compositions of phengite is higher than 0.20 GPa. Summing up the available geothermobarometric information, the *D2* metamorphic condition can be determined as T > 400°C and P > 0.20 GPa. So, the *D2* metamorphic event probably took place at a temperatures greater than those of the *D1* phase.

The coexistence of type 1 and 2 twins (Burkhard 1993) in calcite grains, recrystallized during the *D3* phase, are indicative of a temperature ranging from 150 to 200°C. Even if no analytical data are available, the structures recognized in the field as well as in thin sections, such as crenulation cleavage generated by pressure solution and reorientation of pre-existing grains mechanisms rather than metamorphic replacement, suggest that the *D3* phase was developed at structural levels higher than those estimated for the *D2* phase.

THE DEFORMATION HISTORY OF THE TACAGUA UNIT

The reconstructions proposed for the southern margin of the Caribbean Plate by Pindell and Barrett (1990), Meschede and Frisch (1998) and Giunta *et al.* (2002, 2003), suggest that the ophiolite sequences found in the Cordillera de la Costa can be interpreted as a fragment of oceanic lithosphere involved in the processes connected with a subduction zone originated since the 'Mid' Cretaceous. In the sample VZ 10, the *D1* phase-related mineralogic assemblage is represented by a relics of clinozoisite, chlorite, quartz and phengite characterized by high celadonitic content. This association has been generally recognized in rocks deformed by accretion in a subduction zone, as reported, for instance, by Faryad and Hoinkes (1999) and Tsujimori (2002). The estimated pressure–temperature metamorphic conditions (339°C < T < 406°C and P > 0.45 Gpa) suggest that accretion took place under relatively high thermal gradient, unusual for a subduction zone. However, this type of metamorphism is no surprise. For instance, the Shimanto zone, Japan, is one of the best investigated accretionary wedge where detailed studies (Ujiie 1997; Nagae & Miyashita 1999) showed that most of the accreted sequences has undergone metamorphism with relatively high values of T. In addition, the Tacagua unit is strictly associated to the Nirgua unit, that is characterized by first deformation phase developed under eclogite-facies metamorphism (1.8–2.2 GPa and 500–700°C) with a high value of T (Sisson *et al.* 1997). In this picture, the Tacagua unit, as well as the Nirgua one, can be interpreted as a slice of oceanic lithosphere first deformed under relatively high thermal gradient during underplating within a subduction zones (Moore & Sample 1988; references therein). The proposed models (e.g. Peacock 1996) suggest that the high thermal gradient originated when young and still hot oceanic lithosphere was involved in subduction zone. Unfortunately, the subsequent intense and pervasive deformation phases prevent accurate reconstruction of the structural features of the *D1* phase, such as the strike of the F1 folds and/or the sense of shear during this phase. The relics of the *D1* phase recognized in the Tacagua unit are too rare and scattered to allow a suitable reconstruction of the geometrical characteristics of this phase.

Estimation of metamorphic temperature during the *D2* phase is consistent with an increase of T between the *D1* and *D2* phases. The following *D3* phase has been acquired during the progressive exhumation as suggested by the temperature conditions during the deformation, lower than that during the *D2* phase.

The features of the *D2* phase, characterized by L2 mineral and stretching lineations showing a N60E trend, indicate displacement roughly parallel to the present-day strike-slip faults that are, in turn, parallel to the plate boundary between the Caribbean and South America Plates. This suggests that the deformation of the Tacagua unit during the *D2* phase was likely acquired in a dextral strike-slip shear zone parallel to the plate boundary, according to the model suggested by Avé Lallemant and Guth (1990) and Avé Lallemant (1997). In this model, along oblique subduction zones, the component of the convergent-rate vector parallel to the plate boundary causes displacements along arc-parallel strike-slip faults and shear zones, which results in the exhumation of eclogite and blueschists assemblages.

In contrast, the F3 folds, with flat-lying axial planes and horizontal fold axes, can be interpreted

as originated from vertical shortening and folding of pre-existing non-horizontal layers. This type of deformation is typical of ductile extensional tectonics (Ratschbacher *et al.* 1989; Froitzheim 1992; Wheeler & Butler 1994). This interpretation is in agreement with the association of the *D3* folds with the low-angle normal shear zones, everywhere characterized by motion normal to the plate boundary. According to Wallis *et al.* (1993), not all the convergent margins need be associated with extensional tectonics. However, the geodynamic setting of the southern margin of the Caribbean Plate shows the features regarded as indicative of extensional tectonics. For instance, the occurrence of large volume of oceanic sequences deformed by underplating, the presence of abrupt downward increases in the metamorphic grade, as that recognized between the Tacagua and Nirgua units, and the evidence of displacement at low structural levels of high pressure metamorphic rocks during convergence strongly suggest the extensional tectonics might represent an active mechanism in the southern margin of Caribbean Plate.

Finally, the *D4* phase is characterized by open folds with steep axial planes that seem to be developed in association with east–west dextral strike-slip faults. These faults are parallel to the plate boundary between the Caribbean and South America Plates, whose relative motion is responsible for the development of the *D4* phase.

Different processes are presented to explain the exhumation of metamorphic rocks in a convergent setting (e.g. Cloos 1982; Platt 1986; McCaffrey 1992; Chemenda *et al.* 1995). Particularly, 'corner flow' models have been recently proposed for the exhumation processes in oblique subduction zones (Iwamori 2003; Takeshita & Yagi 2004). These models are essentially based on the observation that during the whole subduction and exhumation process, both subduction-flow and exhumation-flow are characterized by lineation-parallel shear dominant flows (Takeshita *et al.* 2005). These flows are interpreted as the down-flow and the counter-flow of a 'corner-flow' system in an accretionary wedge.

In contrast, the deformation history of the Tacagua unit consists of alternating deformation phases characterized by strike-slip (*D2* and *D4* phases) and pure extensional tectonics (*D3* phase), with displacement directions, respectively, parallel (*D2* and *D4* phases) and normal (*D3* phase) to plate boundary. Furthermore, the 'corner-flow' model appears to be a possible mechanism to explain the occurrence of high-pressure tectonic blocks in mélange, but not the exhumation of large coherent terrains (Platt 1993).

No data are available to constrain the age of the deformations detected in the Tacagua unit. However, the geological mapping provides evidence that the *D3* phase affects also the tectonic boundaries between the Tacagua and Nirgua units producing map-scale structures in which all the oceanic units of the La Costa Metamorphic Suite are folded together. The *D3* phase identified in the Tacagua unit can be correlated with the *D1*d and *D1*e phases recognized in the Nirgua unit by Sisson *et al.* (1997). These phases are characterized by the same metamorphic conditions and both are the result of extensional tectonics. The available data for the Nirgua unit allow to propose a 37/35 Ma (Middle to Late Eocene) age for these phases. Consequently, the *D3* phase in the Tacagua unit can be referred to Middle to Late Eocene timespan, whereas the *D1* and *D2* phases can be regarded as pre-Middle Eocene in age, probably developed during the 'Mid' to Late Cretaceous timespan.

The Nirgua and Tacagua units, even if affected by different pressure–temperature peak metamorphic conditions, were probably deformed in the same geodynamic setting, i.e. a subduction zone. In addition, these units show different peak metamorphic conditions connected with different depth of accretion, deeper for the Nirgua unit and shallower for the Tacagua unit. During the exhumation, the Tacagua and Nirgua units were coupled only after the development of the *D2* phase, according to the structural evidences of the tectonic boundary deformed by the *D3* phase. Their coupling occurred probably in a timespan between the *D2* and *D3* phases during the progressive exhumation of the Tacagua and Nirgua units.

GEODYNAMIC IMPLICATIONS

In the geodynamic reconstructions proposed for the Caribbean area (e.g. Burke 1988; Pindell *et al.* 1988; Ross & Scotese 1988; Morris *et al.* 1990; Pindell 1993; Meschede & Frisch 1998; Giunta *et al.* 2002), the high pressure–low temperature ophiolites from northern Venezuela are interpreted as a remnants of the Proto-Caribbean oceanic lithosphere involved in the subduction zone located at the northwestern corner of the South America Plate in the Early Cretaceous time. The main features of the subduction zone such as its dip, the dip direction, etc. remain undetermined, as a result of the lack of reliable geological data. From the Mid-

Cretaceous period, the evolution of the Caribbean area was dominated by eastward motion of the Caribbean plateau connected with the opening of the South Atlantic Oceanic Basin and the consequent northwestward relative movement of the South America Plate. The eastward drifting of the Caribbean Plate was associated in its eastern margin with the development of an approximately north–south-trending, west-dipping subduction zone where the proto-Caribbean/Atlantic oceanic crust was underthrust below the thickened Caribbean plateau. This subduction is associated to well-developed calcalkaline arc whose magmatism started in the Late Cretaceous time (Beets *et al.* 1984; Sinton *et al.* 1998; Beccaluva *et al.* 1999; White *et al.* 1999; Giunta *et al.* 2002; references therein). In this picture, both the northern and southern boundaries of the Caribbean Plate became characterized by lateral displacement leading to large-scale oblique convergence associated with development of east–west-trending subduction zones (Meschede & Frisch 1998; Sinton *et al.* 1998; Giunta *et al.* 2002; and references therein). In the upper plate of these subduction zones, development of strike-slip faults systems, dismembering in multiple terranes of the pre-existing fore- and back-arc complexes as well as continental block rotation in the upper plate are proposed as result of the strain partitioning of the oblique convergence (Avé Lallemant & Guth 1990; Pindell & Barrett 1990; Avé Lallemant 1997; Meschede & Frisch 1998; Smith *et al.* 1999; Audemard & Audemard 2002; Giunta *et al.* 2002). According to this reconstruction, several lines of geological evidence indicate that the whole history of the Caribbean southern margin has been dominated by an oblique convergence since the Mid-Cretaceous. Similar evidence can be also recognized in the Tacagua unit.

Even if roughly estimated, the pressure–temperature metamorphic conditions during the *D1* phase, seems to be consistent with the involvement of the Tacagua unit in a subduction zone. In addition, the Tacagua unit is characterized by *D2* and *D4* phases developed in a tectonic setting characterized by displacement parallel to plate boundary. Consequently, both these phases, even if developed at different structural level, were connected to a tectonics dominated by strike-slip motion. By contrast, the *D3* phase was probably acquired in a pure extensional setting. This alternation of deformation phases developed in both strike-slip and pure extensional tectonics was acquired during the same oblique convergence, as a result of continuous eastward drifting of the Caribbean Plate since Mid-Cretaceous. This interpretation is also supported by the structural data provided for the ophiolitic units from Cordillera de la Costa by Avé Lallemant (1997) in the Araya peninsula and by Sisson *et al.* (1997) and Avé Lallemant and Sisson (2005) in the Puerto Cabello area, respectively, located eastward and westward of the study area.

Physical modeling (e.g. Chemenda *et al.* 2000) has shown that the strain partitioning is an active mechanism in the subduction zone characterized by oblique convergence. Strain partitioning consists of the accommodation of the oblique plate convergence by thrusting normal to the arc and along-trench displacement of the upper plate leading to the development of strike-slip faults in the fore- and back-arc zones. The strain partitioning is an active mechanism in oblique subduction zones when the interplate friction is high. By contrast, when the interplate friction is low the extension in fore- and back-arc zones is prevailing, with development of low- and high-angle normal faults, parallel to the strike of the trench, leading to exhumation of high pressure–low temperature metamorphic rocks of the accretionary wedge. Physical modeling suggests that the occurrence in the fore- and back-arc zones of strike-slip faults and extension are conflicting processes. Changes in value of interplate friction is likely to be influenced by the lubricating effect of unconsolidated sediments dragged in the subduction zone, the dynamics of the fluids along the decollement zone below the accretionary wedge, the mineralogical transformation of material within the interplate zone, etc. (Molnar & England 1990; Cloos & Shreve 1996; Peacock 1996). However, the most effective parameter which is able to strongly modify the interplate friction is the morphology of the subducting plate. According to Lallemand *et al.* (1994) and Chemenda *et al.* (2000), the subduction of an oceanic crust with a rugged morphology inherited by slow-spreading ridge processes or characterized by oceanic seamounts and/or thickened crust zones can produce an increase in the interplate friction. This increase of the interplate friction is able to modify the strain partitioning, and consequently, the tectonic processes become active in the upper plate. In this way, alternation of postaccretion, extensional and strike-slip deformations detected in the Tacagua unit can be thus interpreted as the result of value change of interplate friction through time in the same geodynamic setting, i.e. an oblique subduction zone. This change can be related to the

subduction of the Caribbean oceanic lithosphere changing features through time. This hyphothesis is supported by the geophysical investigations on the present-day crustal structure of the Caribbean Sea. In this area, the oceanic crust shows a composite seismic structure with change in thickness from 5 to 20 km, a relief that is well in excess of typical oceanic crust (e.g. Mauffrét & Leroy 1997). For instance, multichannel seismic profiles across the Colombia Basin, located in the southeastern corner of the Caribbean Sea, show a crustal structure mainly represented by an oceanic plateau characterized by a thickness at least twice of a typical oceanic crust (Bowland & Rosencratz 1988). However, the Colombia Basin is bordered by an oceanic crust with a normal thickness that represents the basement upon which the plateau was constructed. Probably, this abrupt thickness change of the Caribbean oceanic crust can be regarded, if involved in a subduction, as a feature able to produce the value change of interplate friction, as required by the alternation of postaccretion, extensional and strike-slip deformations detected in the Tacagua unit.

CONCLUSIONS

The Tacagua unit, cropping out in the northern Cordillera of Venezuela, is characterized by a metamorphosed ophiolite sequence with MORB geochemical affinity that includes metaserpentinites, metagabbros and metabasalts. This sequence is topped in turn by a metasedimentary cover consisting of calcschists alternating with pelitic and psammitic schists, whose protoliths were probably represented by deep-sea hemipelagic and turbiditic deposits.

The structural history consists of four deformation phases, *D1* to *D4*. The occurrence of Si-rich phengite, chlorite, clinozoisite and quartz as mineral relics that developed during the *D1* phase, suggests involvement of the Tacagua unit in the processes connected with a subduction zone. As suggested by the structural evidence, the Tacagua unit can be regarded as a tectonic unit accreted by underplating at the base of the accretionary wedge connected with the subduction zone. The following *D2* phase is characterized by isoclinal folds associated with a well-developed foliation and mineral lineation. The *D2* phase was developed at higher temperature conditions than the *D1* phase. The *D3* and *D4* phases, characterized by a similar temperatures and pressures decrease, can be regarded as achieved during the exhumation history. The structural features of these phases indicate alternation of deformation phases characterized by displacement parallel (*D2* and *D4* phases) and normal (*D3* phase), respectively, to the boundary between the Caribbean and South America Plates. On the whole, the geological evidence suggests that the evolution of the Tacagua unit was acquired in a setting dominated by oblique convergence as also suggested by the geodynamic reconstructions proposed for the southern margin of the Caribbean Plate (Avé Lallemant & Guth 1990; Pindell & Barrett 1990; Avé Lallemant 1997; Meschede & Frisch 1998; Smith *et al.* 1999; Giunta *et al.* 2002; Avé Lallemant & Sisson 2005). The same conclusions are drawn, for instance, about the post-Eocene tectonic setting of Venezuela and neighboring areas by Audemard and Audemard (2002). Consequently, the whole evolution of the southern margin of the Caribbean Plate can be envisaged as developed in a long-lived, oblique convergence setting, in which alternance of strike-slip, pure compressional or pure extensional tectonics can be envisaged. One of the mechanisms able to explain this alternace is the strain partitioning controlled by change of interplate friction value, probably resulting from the composite structure of the Caribbean oceanic crust characterized by abrupt change in thickness, as also today observed (e.g. Mauffrét & Leroy 1997).

ACKNOWLEDGEMENTS

This research was supported by C.N.R (Istituto di Geoscienze e Georisorse) and by M.I.U.R (Project COFIN 2000 'Tectono-magmatic significance and structural evolution of Mesozoic ophiolites from the deformed margins of the Caribbean Plate' & Project COFIN 2003 'Tectonic processes in fossil accretionary prism and comparison with modern analogs'). The research was carried out in the framework of the IGCP-433 'Caribbean plate tectonics'.

REFERENCES

AUBOIN J., BLANCHET R., STEPHAN J. & TARDY M. 1977. Tethis (Mèsogèe) et Atlantique: Donnèe de la gèologie. *Compte Rendus Acadèmie de Science* **285**, 1025–8.

AUDEMARD F. E. & AUDEMARD F. A. 2002. Structure of the Merida Andes, Venezuela: relations with the

south America–Caribbean geodynamic interaction. *Tectonophysics* **345**, 299–327.

AVÉ LALLEMANT H. G. 1997. Transpression, displacement partitioning, and exhumation in the eastern Caribbean/South America plate boundary zone. *Tectonics* **16**, 272–89.

AVÉ LALLEMANT H. G. & GUTH R. 1990. Role of extensional tectonics in exhumation of eclogites and blueschists in an oblique subduction setting: Northeast Venezuela. *Geology* **18**, 950–3.

AVÉ LALLEMANT H. G. & SISSON V. B. 2005. Exhumation of eclogites and blueschists in northern Venezuela: Constraints from kinematic analyses of deformation structures. *Geological Society of America, Special Paper* **394**, 193–206.

BECCALUVA L., COLTORTI M., GIUNTA G. *et al.* 1996. Cross sections through the ophiolitic units of the southern and northern margins of the Caribbean plate in Venezuela (Northern Cordilleras) and central Cuba. *Ofioliti* **21**, 85–103.

BECCALUVA L., CHINCHILLA A. L., COLTORTI M., GIUNTA G., SIENA F. & VACCARO C. 1999. The S. Elena-Nicoya Ophiolitic Complex in Costa Rica, and its geodynamic implications for the Caribbean Plate evolution. *European Journal of Mineralogy* **11**, 1091–107.

BEETS D. J., MARESCH W. V., KLAVER G. T. *et al.* 1984. Magmatic rock series and high-pressure metamorphism as constraints on the tectonic history of the southern Caribbean. *In* Bonini W. E., Hargraves R. B. & Shagam R. (eds). *The Caribbean–South America Plate Boundary and Regional Tectonics, Geological Society of America, Memoir* 162, 95–130.

BOWLAND C. L. & ROSENCRATZ E. 1988. Upper crustal structure of the Western Colombian basin, Caribbean sea. *Geological Society of America Bulletin* **100**, 534–46.

BURKE K. 1988. Tectonic evolution of the Caribbean. *Annual Reviews in Earth and Planetary Sciences* **16**, 201–30.

BURKHARD M. 1993. Calcite twins, their geometry, appearance and significance as stress-strain markers and indicators of tectonic regime: A review. *Journal of Structural Geology* **15**, 351–68.

CHEMENDA A. I., MATTAUER M., MALAVIEILLE J. & BOKUN A. N. 1995. A mechanism for syn-collisional rock exhumation and associated normal faulting; results from physical modelling. *Earth and Planetary Science Letters* **132**, 225–32.

CHEMENDA A., LALLEMAND S. & BOKUN A. 2000. Strain partitioning and interplate friction in oblique subduction zones: constraints provided by experimental models. *Journal of Geophysical Research* **105-B3**, 5567–81.

CLOOS M. 1982. Flow melanges; numerical modeling and geologic constraints on their origin in the Franciscan subduction complex, California. *Geological Society of America Bulletin* **93**, 330–44.

CLOOS M. & SHREVE R. L. 1996. Shear zone thickness and seismicity of Chilean- and Mariana-type subduction zones. *Geology* **24**, 107–10.

DENGO G. 1985. Mid America: Tectonic setting for the Pacific margin from Southern Mexico to North Western Colombia. *In* Nairn A. E. M., Stehli F. G. & Uyeda S. (eds). *The Ocean Basin and Margins* **7**, 15–37.

DENGO G. & CASE J. H. (eds). 1990. The Caribbean region. Geological Society of America, Boulder.

ELLERO A., MARRONI M., PADOA E., PANDOLFI L. & URBANI F. 2001. Deformation history of the blueschist-facies sequences from the Villa de Cura unit (Northern Venezuela). *Ofioliti* **26**, 479–83.

FARYAD S. W. & HOINKES G. 1999. Two contrasting mineral assemblages in the Meliata blueschists, Western Carpathians. *Slovakia Mineralogical Magazine* **63–4**, 489–501.

FRISCH W., MESCHEDE M. & SICK M. 1992. Origin of the Central American ophiolites: Evidences from paleomagnetic results. *Geological Society of America Bullettin* **104**, 1301–14.

FROITZHEIM N. 1992. Formation of recumbent folds during synorogenic crustal extension (Austroalpine nappes, Switzerland). *Geology* **20**, 923–6.

GIUNTA G. 1993. Los márgenes mesozoicos de la Placa Caribe: Problemáticas sobre nucleación y evolución. *Memoria, Congreso Colombiano de Geología, 6th, Medellín, Sociedad Geológica Colombiana* **3**, 1–14.

GIUNTA G., BECCALUVA L., COLTORTI M., SIENA F. & VACCARO C. 2002. The southern margin of the Caribbean plate in Venezuela: tectono-magmatic setting of the ophiolitic units and kinematic evolution. *Lithos* **63**, 19–40.

GIUNTA G., MARRONI M., PADOA E. & PANDOLFI L. 2003. Geological constraints for the geodynamic evolution of the southern margin of the Caribbean plate. *In* Bartolini C., Buffler R. T. & Blickwede J. F. (eds). *The Circum-Gulf of Mexico and the Caribbean*, Vol. 79, pp. 104–25. AAPG Memoir. American Association of Petroleum Geologists, Tulsa.

ITURRALDE-VINENT M. 1994. Cuban geology: a new plate tectonic synthesis. *Journal of Petroleum Geology* **17**, 38–70.

IWAMORI H. 2003. Viscous flow and deformation of regional metamorphic belts at convergent plate boundaries. *Journal of Geophysical Research* **108**, 2321. doi: 10.1029/2002JB001808.

KERR A. C., ITURRALDE-VINENTE M. A., SAUNDERS A. D., BABBS T. L. & TARNEY J. 1999. A new plate tectonic model for the Caribbean: implications from a geochemical reconnaissance of Cuban mesozoic volcanic rocks. *Geological Society of America Bullettin* **111**, 1581–99.

LALLEMAND S. E., SCHURLE P. & MALAVIELLE J. 1994. Coulomb theory applied to accretionary or nonaccretionary wedges: possible causes for tectonic

erosion and/or frontal accretion. *Journal of Geophysical Research* **99**, 12033–55.

LEAKE B. E., WOOLEY A. R., ARPS C. E. S., *et al.* 1997. Nomenclature of amphiboles: Report of subcommittee on amphiboles of the International Mineralogical Association, commission on new minerals and mineral names. *Canadian Mineralogist* **35**, 219–46.

MCCAFFREY R. 1992. Oblique plate convergence, slip vectors, and forearc deformation. *Journal of Geophysical Research* **97**, 8905–15.

MASSONNE H. J. & SCHREYER W. 1987. Phengite geobarometry based on the limitino assemblage with K-feldspar, phlogopite, and quartz. *Contribution to Mineralogy and Petrology* **96**, 212–24.

MASSONNE H. J. & SZPURSKA Z. 1997. Thermodynamic properties of white micas on the basis of high-pressure experiments in the systems K_2O-MgO-Al_2O_3-SiO_2-H_2O and K_2O-FeO-Al_2O_3-SiO_2-H_2O. *Lithos* **41**, 229–50.

MAUFFRÉT A. & LEROY S. 1997. Seismic stratigraphy and structure of the Caribbean igneous province. *Tectonophysics* **283**, 61–104.

MÉNDEZ J. & NAVARRO E. 1987. Caracterizatión geoquímica de las metalavas de la Formación Tacagua. *Memorias 1ras. Jornadas de Investigatión en Ingeniería- Fac. Ing. UCV* **1**, 44–7.

MESCHEDE M. & FRISCH W. 1998. A plate-tectonic model for Mesozoic and Early Cenozoic evolution of the Caribbean plate. *Tectonophysics* **296**, 269–91.

MOLNAR P. & ENGLAND P. C. 1990. Temperature, heat flux and frictional stress near major thrust faults. *Journal of Geophysical Research* **95**, 4833–56.

MOORE J. C. & SAMPLE J. 1988. Mechanism of accretion at sediment-dominated subduction zones: consequence for the stratigraphic record and accretionary prism hydrogeology. *Memorie Della Società Geologica Italiana* **31**, 107–18.

MORRIS A. E. L., TARNEY I., MEYERHOFF H. A. & MEYERHOFF A. A. 1990. Tectonic evolution of the Caribbean region; Alternative hypothesis. *In* Dengo G. & Case J. E. (eds). *The Caribbean Region: Boulder, Colorado, Geological Society of America, the Geology of North America* H, 433–57.

NAGAE S & MIYASHITA O. 1999. Low-P/T type metamorphism and deformation of the northern Shimanto Belt, Kyushu, southwest Japan. *Memoirs of the Geological Society of Japan* **52**, 255–72 (in Japanese with English abstract).

OSTOS M. 1990. Evolucion tectonica del margen Sur-Central del Caribe, basados en datos geoquìmicos. *GEOS (Caracas, Escuela de Geologìa Y Minas, Universidad Central de Venezuela)* **30**, 1–294.

OSTOS M., YORIS F. & AVÉ LALLEMANT H. G. 2005. Overview of the southeast Caribbean–south America plate boundary zone. *Geological Society of America, Special Paper* **394**, 53–90.

OTSUKI M. & BANNO S. 1990. Prograde and retrograde metamorphism of hematite-bearing basic schists in the Sambagawa belt in central Shikoku. *Journal of Metamorphic Geology* **8**, 425–39.

PEACOCK S. M. 1996. Thermal and petrological structure of subduction zones. *In* Bebout G., Scholl D. W, Kirby S. H. & Platt J. P (eds). *Subduction: Top to Bottom, Geophycal Monogrophy Series* 96, 119–33.

PINDELL J. L. 1993. Regional synopsis of Gulf of Mexico and Caribbean evolution. *In* Pindell J. L. & Perkins B. F. (eds). *Mesozoic and Early Cenoizoic Development of the Gulf of Mexico and Caribbean Region: A Context for Hydrocarbon Exploration, Gulf Coast Section, SEMP Foundation 13th Annual Research Conference: Houston, Texas, SEMP (Society for Sedimentary Geology) Foundation*, pp. 251–74. Society for Sedimentary Geology Foundation, Texas.

PINDELL J. L. & BARRETT S. F. 1990. Geological evolution of the Caribbean region: a plate-tectonic perspective. *In* Dengo G. & Case J. E. (eds). *The Caribbean Region: Boulder, Colorado, Geological Society of America, the Geology of North America* H, 339–74.

PINDELL J. L., CANDE S. C., PITMAN W. C. III. *et al.* 1988. A plate-kinematic framework for models of Caribbean evolution. *Tectonophysics* **155**, 121–38.

PLATT J. P. 1986. Dynamics of orogenic wedges and the uplift of high-pressure metamorphic rocks. *Geological Society of America Bulletin* **97**, 1037–53.

PLATT J. P. 1993. Exhumation of high-pressure rocks: a review of concepts and processes. *Terra Nova* **5**, 119–33.

RAMSAY J. G. 1967. *Folding and Fracturing of Rocks.* Mc Graw, Hill, New York.

RATSCHBACHER L., FRISCH W., NEUBAUER F., SCHMID S. M. & NEUGEBAUER D. 1989. Extension in compressional orogenic belts: The Eastern Alps. *Geology* **17**, 404–7.

RÉVILLON S., HALLOT E., ARNDT N. T., CHAUVEL C. & DUNCAN R. A. 2000. A complex history for the Caribbean Plateau: petrology, geochemistry and geochronology of the Beata Ridge, South Hispaniola. *Journal of Geology* **108**, 641–61.

ROSS M. I. & SCOTESE C. R. 1988. A hieratical tectonic model of the Gulf of Mexico and Caribbean Region. *Tectonophysics* **155**, 139–68.

ROWLAND S. M. & DUEBENDORFER E. M. 1994. *Structural Analyses and Synthesis*. Blackwell Scientific Publication, Boston.

SINTON C. W., DUNCAN R. A., STOREY M., LEWIS J. & ESTRADA J. J. 1998. An oceanic flood basalt province within the Caribbean Plate. *Earth and Planetary Sciences Letters* **155**, 221–35.

SISSON V. B., EVREN ERTAN I. & AVE' LALLEMANT H. G. 1997. High-pressure (–2000 MPa) kyanite- and glaucophane-bearing pelitic schist and eclogite from Cordillera de la Costa Belt, Venezuela. *Journal of Petrology* **38**, 65–83.

SMITH C. A., SISSON V. B., AVÉ LALLEMANT H. G. & COPELAND P. 1999. Two contrasting pressure-temperature paths in the Villa de Cura blueschist belt, Venezuela: possible evidence for Late Cretaceous initiation of subduction in the Caribbean. *Geological Society of America Bulletin* **111**, 831–48.

STEPHAN J. F., MERCIER DE LEPINAY B., CALAIS E. *et al.* 1990. Paleogeodynamic maps of the Caribbean: 14 steps from Lias to present. *Bullettin de la Societé Géologique de France* 8, 915–19.

TAKESHITA T. & YAGI K. 2004. Flow patterns during exhumation of the Sambagawa metamorphic rocks, southwest Japan, caused by brittle-ductile, arc-parallel extension. *In* Grocott J., Mccaffrey K., Taylor K. & Tikoff B. (ed.). *Vertical Coupling and Decoupling in the Lithosphere.* Geological Society, London. Special Publications. **227**, 279–96.

TAKESHITA T., ISHII K. & KANAGAWA K. 2005. Flow kinematics in the deeper part of a subduction channel, as inferred from inclusion trails in plagioclase porphyroblasts from the Sambagawa metamorphic rocks, south-west Japan. *Journal of Metamorphic Geology* **23**, 279–94.

TALUKDAR S. & LOUREIRO D. 1982. Geología de una zona ubicada en el segmento norcentral de la Cordillera de la Costa, Venezuela: metamorfismo y deformatión. Evolución del margen septentrional de Sur América en el marco de la tectónica de Placas. *GEOS (Caracas, Escuela de Geología Y Minas, Universidad Central de Venezuela)* **27**, 15–76.

TSUJIMORI T. 2002. Prograde and Retrograde P-T Paths of the Late Paleozoic Glaucophane Eclogite from the Renge Metamorphic Belt, Hida Mountains, Southwestern Japan. *International Geology Review* **44**, 797–818.

UJIIE K. 1997. Off-scraping accretionary process under the subduction of young oceanic crust: the Shiamanto Belt of Okinawa Island, Ryukyu Arc. *Tectonics* **16**, 305–22.

URBANI F. 1999. Revìsion de la unidades de rocas ìgneas y metamorficas de la Cordillera de la Costa, Venezuela. *GEOS (Caracas, Escuela de Geologìa Y Minas, Universidad Central de Venezuela)* **33**, 1–170.

URBANI F. & RODRÍGUEZ J. A. 2003. Atlas geológico de la Cordillera de la Costa, Venezuela. Caracas: Edic. *FUNVISIS y University of Central Venezuela, 148 Maps* **1**, 25.000.

VELDE B. 1967. Si^{4+} content of natural phengites. *Contributions to Mineralogy and Petrology* **14**, 250–8.

VIDAL O, PARRA T, TROTET F. 2001. A thermodynamic model for Fe-Mg aluminous chlorite using data from phase equilibrium experiments and natural pelitic assemblages in the 100–600°C, 1-25 kbar P-T range. *American Journal of Science* **301**, 557–92.

WALLIS S. R., PLATT J. P. & KNOTT S. D. 1993. Recognition of syn-convergence extension in accretionary wedges with examples from the Calabrian arc and the eastern Alps. *American Journal of Science* **293**, 463–95.

WHEELER J. & BUTLER R. W. H. 1994. Criteria for identifying structures related to true extension in orogens. *Journal of Structural Geology* **16**, 1023–7.

WHITE R. V., TARNEY J., KERR A. C. *et al.* 1999. Modification of an oceanic plateau, Aruba, Dutch Caribbean: implication for the generation of continental crust. *Lithos* **46**, 43–68.